

## Article

# Towards a Healthy Car: UVC LEDs in an Automobile's HVAC Demonstrates Effective Disinfection of Cabin Air

Richard M. Mariita <sup>1,\*</sup> , James H. Davis <sup>2</sup>, Michelle M. Lottridge <sup>1</sup>, Rajul V. Randive <sup>2</sup>, Hauke Witting <sup>3</sup> and Johannes Yu <sup>3</sup>

<sup>1</sup> Product Engineering Department, Crystal IS Inc., an Asahi Kasei Company, 70 Cohoes Avenue, Green Island, NY 12183, USA

<sup>2</sup> Applications Engineering Department, Crystal IS Inc., an Asahi Kasei Company, 70 Cohoes Avenue, Green Island, NY 12183, USA

<sup>3</sup> Business Development Automotive, Asahi Kasei Europe GmbH, Fringsstraße 17, 40221 Düsseldorf, Germany

\* Correspondence: richard.mariita@cisuv.com; Tel.: +1-(518)-478-8018

**Abstract:** Vehicle Heating, ventilation, and air conditioning (HVAC) systems can accumulate and recirculate highly infectious respiratory disease agents via aerosols. Integrating Ultraviolet Subtype C (UVC) light-emitting diodes (LEDs) to complement automobile HVAC systems can protect occupants from developing allergies, experiencing inflammatory problems, or acquiring respiratory infectious diseases by inactivating pathogenic microorganisms. UVC can add little to no static pressure with minimal space, unlike mercury lamps which are larger and heavier. Additionally, UVC LEDs are effective at low voltage and have no mercury or glass. While previous experiments have shown UVC LED technology can reduce bacteriophage Phi6 concentrations by 1 log in 5 min (selected as the average time to clean the cabin air), those studies had not positioned LED within the HVAC itself or studied the susceptibility of the surrogate at the specific wavelength. This study aimed to assess the disinfection performance of UVC LEDs in automotive HVAC systems and determine the dose–response curve for bacteriophage Phi6, a SARS-CoV-2 surrogate. To achieve this, UVC LEDs were installed in a car HVAC system. To determine inactivation efficacy, a model chamber of 3.5 m<sup>3</sup>, replicating the typical volume of a car, containing the modified automobile HVAC system was filled with bacteriophage Phi6, and the HVAC was turned on with and without the UVC LEDs being turned on. The results revealed that HVAC complemented with UVC reduced bacteriophage Phi6 levels significantly more than the HVAC alone and reduced the viral concentration in the cabin by more than 90% in less than 5 min. The performance after 5 min is expected to be significantly better against SARS-CoV-2 because of its higher sensitivity to UVC, especially at lower wavelengths (below 270 nm). HVAC alone could not achieve a 90% viral reduction of bacteriophage Phi6 in 15 min. Thus, applying UVC LEDs inside an HVAC system is an effective means of quickly reducing the number of aerosolized viral particles in the chamber, by inactivating microorganisms leading to improved cabin air quality.

**Keywords:** automobile; bacteriophage Phi6; bioaerosols; HVAC; susceptibility; SARS-CoV-2; UVC LEDs; vehicle



**Citation:** Mariita, R.M.; Davis, J.H.; Lottridge, M.M.; Randive, R.V.; Witting, H.; Yu, J. Towards a Healthy Car: UVC LEDs in an Automobile's HVAC Demonstrates Effective Disinfection of Cabin Air. *Atmosphere* **2022**, *13*, 1926. <https://doi.org/10.3390/atmos13111926>

Academic Editors: Xingwang Zhao, Junzhou He and Zhipeng Deng

Received: 30 September 2022

Accepted: 16 November 2022

Published: 18 November 2022

**Publisher's Note:** MDPI stays neutral with regard to jurisdictional claims in published maps and institutional affiliations.



**Copyright:** © 2022 by the authors. Licensee MDPI, Basel, Switzerland. This article is an open access article distributed under the terms and conditions of the Creative Commons Attribution (CC BY) license (<https://creativecommons.org/licenses/by/4.0/>).

## 1. Introduction

Heating, ventilation, and air conditioning (HVAC) systems in cars, trucks and buses have become standard for decades, although with health implications because of the accumulation and recirculation of microorganisms, including those that cause infectious respiratory diseases [1]. Mold (fungi), bacteria, pollen and proteins can deposit and grow on filters, heating and cooling coils, and surfaces in the HVAC system [2]. These microbes can cause respiratory infectious diseases, allergic reactions and cancer [3]. In addition to their accumulation in the HVAC systems, recirculation of bio-aerosols within an automobile cabin is of public health concern. Bioaerosols can include viruses like SARS-CoV-2,

MERs-CoV, and H1N1, which are responsible for major global disease outbreaks [4,5]. Poor cabin air quality can also be due to mold (fungi) and bacteria that produce mycotoxins, endotoxins,  $\beta$ -glycans and other allergens [3]. The mold that is commonly transmitted via bio-aerosols includes *Scedosporium apiospermum*, *Aspergillus fumigatus*, *Fusarium moniliforme* and *Mucorales* spp. [6]. These mold species can cause localized and systemic organ infections, acute toxicity, hypersensitivity, and other respiratory complications [6]. Pathogenic bacteria such as *Bordetella pertussis*, *Bacillus anthracis*, *Corynebacterium diphtheriae* and *Neisseria meningitidis* can cause the collapse of the respiratory system and neurological abnormalities are also transmissible through bio-aerosols [7].

Since it has been speculated that the air inside car cabins is worse than the outside air [8] and because Americans spend an hour per day in their car [9] managing air quality challenges is especially important. Public health risks associated with bioaerosols have gained significant attention due to the COVID-19 pandemic, caused by SARS-CoV-2 as revealed by recent surveys which show that car occupants now care about whether their vehicles and their HVAC systems are clean [10,11]. To reduce the rates of transmission of SARS-CoV-2. However, the usefulness of polyvinyl chloride (PVC) film barriers and disinfectants are limited against aerosols as they can diffuse everywhere. Rolling down windows or switching to external air can help, but when it is raining, snowing, hot, cold, loud or if external air quality is poor due to exhaust gases, dust, etc., the use of HVAC is the best alternative for the comfort and safety of the car occupants. Additionally, rolled-down windows, especially on highways will decrease fuel economy, because of the higher drag coefficient associated with wind resistance [12]. This consequently will also increase the automobile's carbon dioxide (CO<sub>2</sub>) footprint [13].

Consequently, there has been increasing interest in innovative technologies to allow HVAC systems to remove or inactivate viral and other particles. Sufficiently aggressive high-efficiency particulate air (HEPA) filters can trap some viral particles but create a significant pressure head [14], consuming more power, lowering flow and increasing noise. Mercury lamps that produce Ultraviolet subtype C (UVC) light have previously been used to disinfect and prevent mold and bacterial growth on HVAC coils, especially in buildings [15]. Studies have also shown that a combination of Ultraviolet-A (UVA) and TiO<sub>2</sub> can disinfect airborne bacteria and viruses [16]. However, mercury lamps are high voltage, contain mercury and glass and often have a large footprint due to being larger and heavier [17], all of which may be prohibitive for vehicles because they will make emergency responses difficult in case of accidents.

Promisingly, UVC light-emitting diodes (LEDs), which are now commercially available, have been shown to inactivate bio-aerosols in vehicles without voltage, glass and mercury risks (Figure 1) [18]. Other technologies such as the use of nanofiber filters can help remove mold, bacteria, and viruses [19], but complementing them with UVC technology the trapped microbial assemblages are inactivated, and they do not multiply in the HVAC system. This will minimize the quantity of trapped microbial particles on the filter, increasing filter lifetime and efficiency. Inactivation using UVC is important as pathogens such as SARS-CoV-2 can remain viable in aerosols for about 3 h and can survive for 24 h on porous surfaces such as cardboard and 72 h on smooth surfaces such as stainless steel and plastic [20].

There have been questions about the design, implementation, and transferability of past research on UVC LEDs in vehicle HVACs. That research did not show how or where a UVC system could fit in a vehicle HVAC system but instead placed the disinfection chamber at the inlet of the HVAC system [18]. It also did not show that this method works with other HVAC systems which may have differences; did not control humidity and did not include data on the SARS-CoV-2 or bacteriophage Phi6 susceptibility at the relevant wavelength. This project aimed to determine the dose–response curve of bacteriophage Phi6, a SARS-CoV-2 air disinfection surrogate and examine the performance of UVC integrated into an automotive HVAC system. To achieve this, we nebulized viral particles into a car surrogate chamber, with air passing through the blower and filter of a car HVAC in one setting and another set with air passing through the blower and filter fitted with UVC.

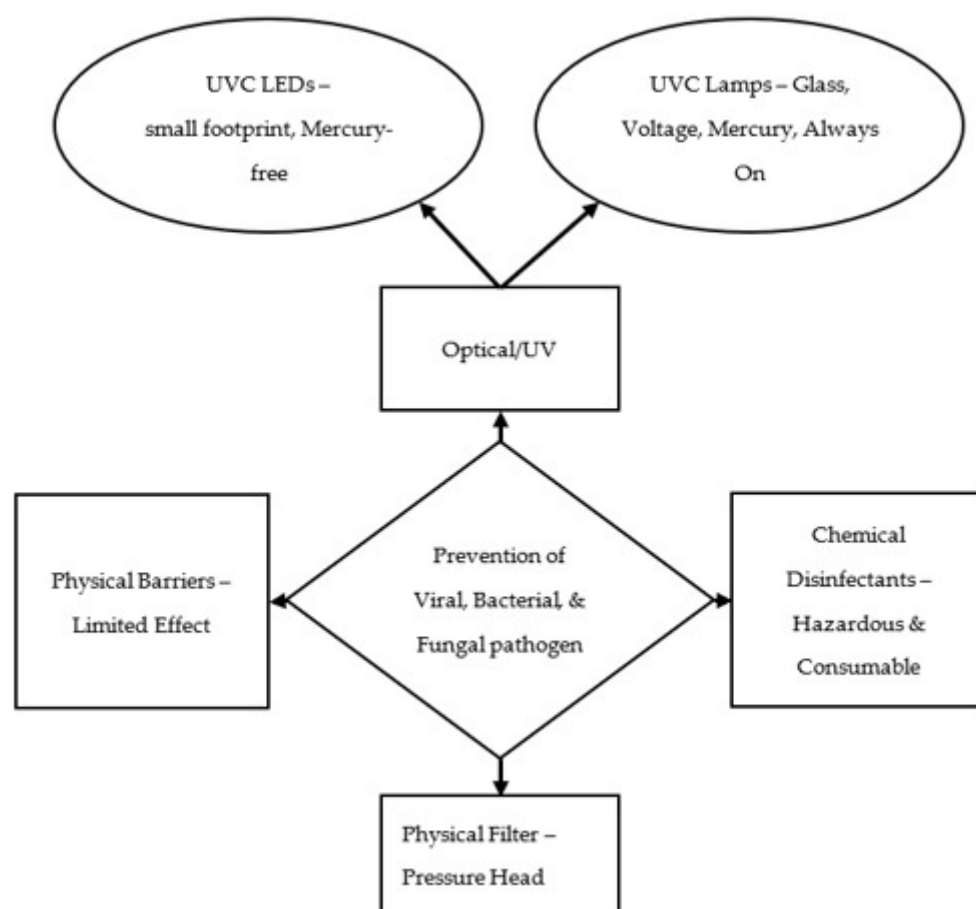


**Figure 1.** A map of the field of prevention of the transmission of airborne pathogens in enclosed spaces with a focus on UVC and weaknesses of competing technologies.

## 2. Materials and Methods

### 2.1. Culture Growth and Preparation of Bacteria and Bacteriophage Strains

Bacteriophage Phi6 (DSM-21518) and its *Pseudomonas syringae* host (DSM 21482) were purchased from the German Collection of Microorganisms and Cell Cultures DSMZ. *Pseudomonas syringae* strain (host for bacteriophage Phi6) was revitalized using 1.5% Tryptic Soy Agar (TSA) and a single pure colony was used to make 10% (v/v) glycerol stocks for long-term storage at  $-80^{\circ}\text{C}$ . Before being used to revitalize bacteriophage Phi6, the *Pseudomonas syringae* host was incubated overnight while shaking at  $120\times g$  rpm at  $28^{\circ}\text{C}$  in Tryptic Soy Broth (TSB). Then, the bacteriophage Phi6 was mixed with the host [21] using the overlay approach (1 mL phage on 10 mL 1.5% TSA, then immediately added 5 mL of 1% TSA maintained at  $50^{\circ}\text{C}$  in a water bath (Julabo, SW22, Seelbach, Germany) prior to the addition of 100  $\mu\text{L}$  of its host at  $\text{OD}_{600}$  of 0.3). The culture plates were incubated for 24 h at  $25\text{--}28^{\circ}\text{C}$ . Then, 5 mL of SM buffer (pH 7.5) (Alfa Aesar, Cat #J61367, Haverhill, MA, USA), containing NaCl,  $\text{MgSO}_4\cdot 7\text{H}_2\text{O}$ , Tris and gelatin was pipetted onto a plate that showed confluent lysis. The plate was slowly rocked for 40 min and the buffer was transferred to a tube for centrifugation at  $4500\times g$  rpm for 10 min. Bacteriophage Phi6 was filtered using sterile  $0.22\text{ }\mu\text{m}$  polycarbonate membrane filters (Sterlitech, SKU PCT0247100, Auburn, WA, USA) before storage at  $4^{\circ}\text{C}$ . Bacteriophage Phi6 concentrations were determined by the plaque assay [22]. For storage, bacteriophage Phi6 was suspended in 40% glycerol and kept at  $-20^{\circ}\text{C}$  as freezer stock.

### 2.2. Set Up and Bacteriophage Phi6 Dose Response Curve

A commercially available Klaran UVC LED (Crystal IS KL265-50V-SM-WD) was mounted to a fan sink (Sunon LA002-001A99DY) on a laboratory stand above a Petri dish

and powered with 500 mA. The spectrum was measured with a spectrograph (Ocean Optics Maya 2000 Pro) and the power was measured with an optometer (Gigahertz X1 MD-37-SC1-4) calibrated at 265 nm. The height was adjusted until the optometer reading showed  $1.00 \text{ mW/cm}^2$  in the center of the inside bottom of the Petri dish. The center of the Petri dish was located at the center of the irradiance by measuring the shadow cast on paper. Then, 1 mL of diluted bacteriophage Phi6 in buffer solution was placed at the center of empty  $100 \times 15 \text{ mm}$  Petri dishes (USA Scientific, Cat #8609-1010, Ocala, FL, USA) and exposed to UVC for each irradiation time.  $100 \text{ }\mu\text{L}$  was then applied on  $500 \text{ }\mu\text{L}$  of host *Pseudomonas syringae* at  $\text{OD}_{600}$  of 0.3 on 1.5% TSA agar in triplicate. Plates were then incubated for 20 h at  $25\text{--}28 \text{ }^\circ\text{C}$ .

### 2.3. Modelling and Simulation of Reaction Chamber

The internal dimensions of the section of the HVAC after the filter & blower but before the rest of the HVAC was measured using calibrated calipers and Modelled using Computer-aided Design (CAD) (Solidworks 2018). Triangular light baffles were added to the inlet and outlet. Then, this design was exported as a STEP file into an optics simulator (Zemax OpticStudio 20.2.2, Kirkland, WA, USA). The internal Barium sulfate ( $\text{BaSO}_4$ ) coating was simulated by approximating the walls as 90% reflective with a 100% Lambertian distribution. A highly reflective sheet of aluminum (Almecco VegaUV) to which the LEDs are attached to was simulated with a plane of 90% reflective 100% specular material. Then, three volumes of size  $1.5 \times 70 \times 10 \text{ mm}$  representing the PCBs (Printed Circuit Boards) coated with  $\text{BaSO}_4$  were simulated with the same coating as the internal volume (Figure 2). Nine UVC LEDs were simulated using ray files obtained with Techno Team's imaging goniometer and available from Crystal IS outputting 56 mW.

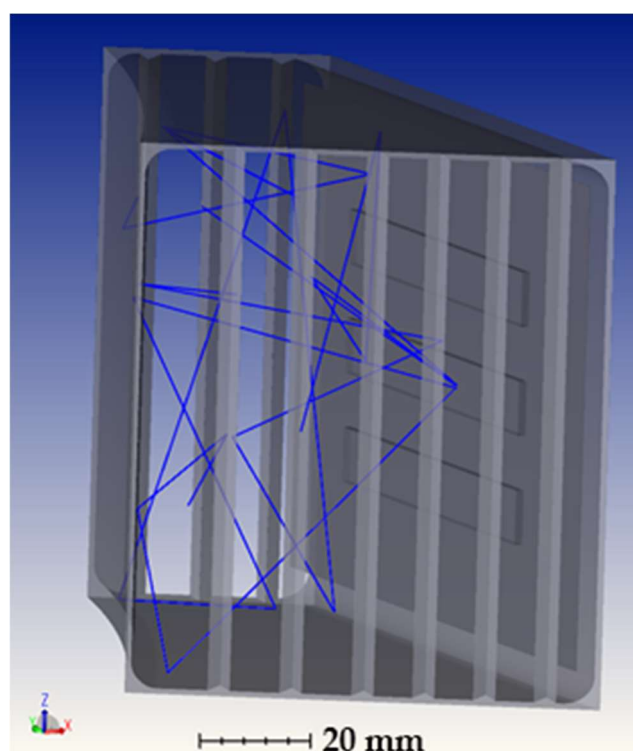


**Figure 2.** The model of the disinfection chamber in Zemax Optic Studio showing the triangular extrusion light baffles, PCB placement and reflectors. One LED is shining showing the way light is scattered inside.

The optical power escaping the outlet was measured for comparison to measured results using a plane detector. A measurement of the internal fluence was made by filling the space with as large a detector volume filling most of the internal volume ( $26 \times 80 \times 96 \text{ mm}$ )



with voxels of side lengths  $4 \times 4.3 \times 4.8$  mm. The fluence ( $I$ ) was then approximated by treating each voxel as a sphere with equivalent volume and calculating the fluence rate with the following formula:

$$I = \frac{P}{2\pi * \sqrt[3]{\frac{3l_1l_2l_3}{4\pi}}} \quad (1)$$

where  $P$  is the flux through the voxel, and  $l_1$ – $l_3$  are the voxel side lengths.

#### 2.4. Bacteriophage Phi6 Air Disinfection Procedure

A chamber was constructed [3] which was composed of 0.5 mm thick PolyVinyl Chloride (PVC) film wrapped around a 1 aluminum extrusion frame with a volume of  $3.5 \text{ m}^3$ . Two brushless mixing fans (Delta Electronics FFC1212DE) were placed inside with one pointed approximately 45 degrees and elevated approximately 18 inches from the floor, while the other was placed with a cardboard shroud and pointed directly upward. This was intended to reduce viral particles from settling for both HVAC only and HVAC + UVC test settings. A humidifier (Safety 1st IH497) and dehumidifier (ProBreeze PB-02-US) were placed inside. Rubber gloves were placed through the PVC film to allow manipulation of materials inside. Power supplies and LIN controller were next to these gloves as was a Craftsman Pressure Pump. The pump was connected to a nebulizer (CH Technologies 6-jet nebulizer). Finally, a sample pump (SKC 901-4011) and gelatin samplers (SKC 225-360) were placed inside near each corner of the enclosure. The layout is shown in Figure 3.

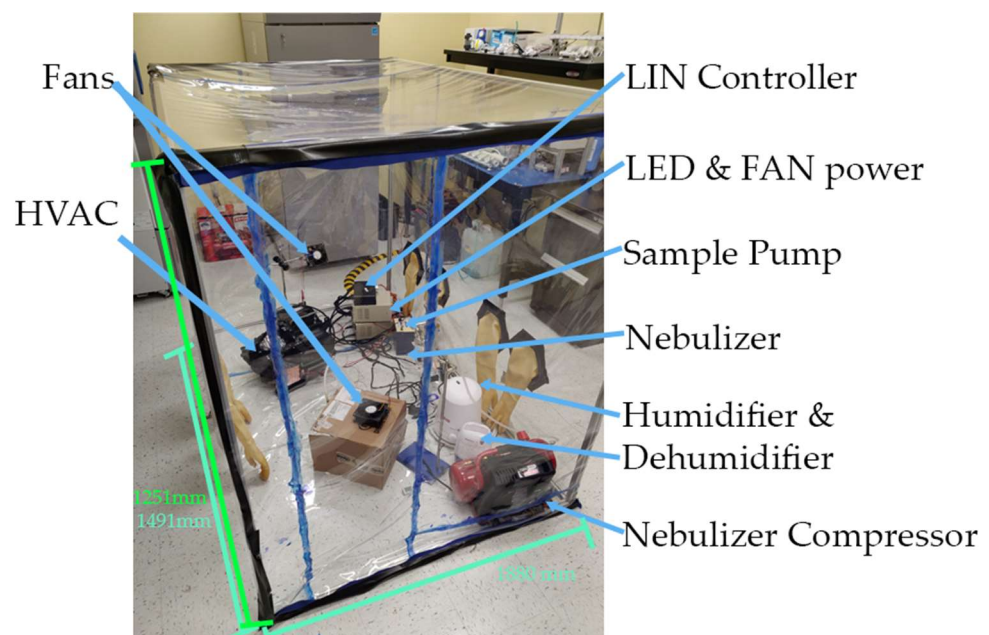


**Figure 3.** The test chamber with labeled components.

The blower and filter component of the HVAC was connected to a custom-built Local Interconnect Network (LIN) controller which controlled and read the Rotations Per Minute (RPM) of the blower. The internal cavity was coated with White Diffuse Reflectance Coating (WRC) (Labsphere AS-02927-000)—which is primarily  $\text{BaSO}_4$  in water. This formed the reaction chamber. Four 3D printer triangular extrusions were placed on the inlet of the reaction chamber and 6 on the outlet spaced approximately 10 mm apart. The inward-facing side of the extrusions were also coated with WRC. A piece of highly reflective aluminum (Alemco VegaUV) sheet was placed with the polished side facing into the chamber covering the straight side wall. Three PCBs with three UVC LEDs (Crystal IS KL265-50V-SM-WD) each were mounted onto the aluminum using thermal paste and M2 screws. All PCBs had constant current circuits to provide LEDs with 500 mA of current. The PCBs were then

coated with WRC except where it would cover or interfere with the LEDs [4]. The final construction is shown in Figure 4.

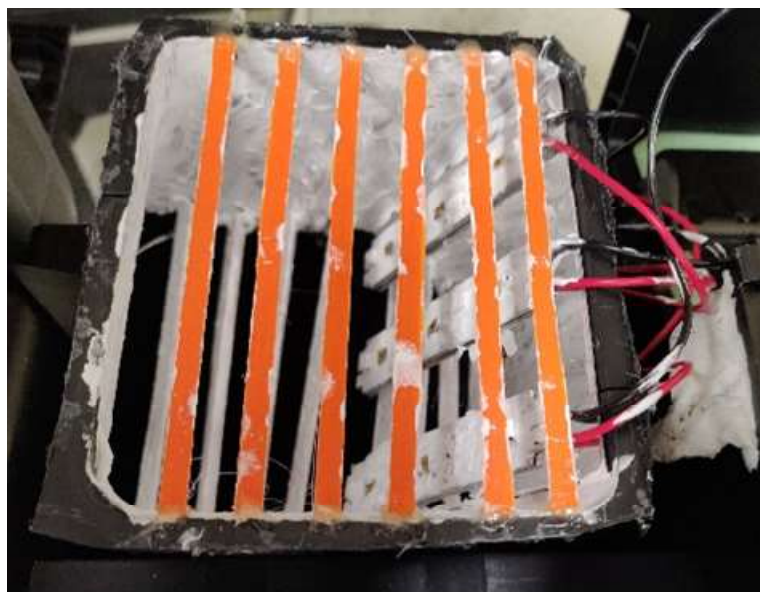


**Figure 4.** The disinfection chamber as built includes the non-ideality of the BaSO<sub>4</sub> coating, the placement of the triangular extrusion and the extent of the coating of the LED PCB.

Between each test and initially, the enclosure was wiped down with 70% ethanol solution and left for more than an hour to decontaminate. An anemometer (BTMeter BT-866A) was used to confirm the air speed of 4.8 m/min such that the flow rate is approximately 250 m<sup>3</sup>/h. The sample pump flow rate through dummy gelatin filters (SKC 225-9551) was measured with a calibrated flow meter (King Instruments 75301112c11) at 24.8 LPM (Liters Per Minute). A solution of 20 mL of bacteriophage Phi6 solution was placed into the nebulizer. The two mixing fans were then run at 8.1 V. The test chamber was then sealed. The humidifier and dehumidifier were then used to adjust the starting humidity to 42% and the temperature was confirmed to be 17.8 °C using HOBO temp/RH logger (Cat #UX100-011A). The humidifier and dehumidifier were then turned off prior to inactivation experiments.

The nebulizer was run for 30 min at 2 bars as read from the pressure pump (Craftsman, Model #:10265). The release of air from the tank reduced pressure from 2 bar to 1.7 bar by the end of the nebulization time. The pressure valve and pump were then turned off and the chamber was allowed to sit for 5 min without nebulization to allow for settling. Then, the SKC flite 4 (Part Number: 901-4011) pulled air through three SKC air samplers connected in parallel through gelatin samplers for 2 min. Gelatin samples were temporarily stored in sterile containers. The HVAC was set to the relevant RPM. In the UVC on condition, the three PCBs (Printed Circuit Boards) were also charged with 24 V at that same time. Samples were taken again after 5, 10, and 15 min. The system was then powered off and the whole system was disconnected from power for decontamination with ethanol.

The bacteriophage Phi6 was prepared using the overlay method: 500 µL of host *Pseudomonas syringae* with OD<sub>600</sub> of 0.3 followed by 5 mL of 1% TSA at 50 °C was added and quickly mixed such that the gelatin filter dissolved and then was poured on top of 10 mL solidified 1.5% TSA in a Petri dish. The samples stayed at room temperature for 30 min to allow for solidification, then incubated at 25–28 °C for 20 h prior to counting. The remainder of the liquid in the nebulizer was measured by graduated cylinder and was consistently between 8 and 8.2 mL.

### 2.5. Statistical Analysis

The counted plaque forming units (PFU) per gel were used to calculate log reduction values (LRV) (Table 1) based on the following formula.

$$LRV = \log_{10}\left(\frac{C_i}{C_f}\right) \quad (2)$$

where  $C_i$  is the number of PFUs from the control gelatin filters (no UVC) and  $C_f$  is the number of PFUs from the test gelatin filters (with UVC).

**Table 1.** Disinfection performance of UVC LEDS fitted into the automobile HVAC system against bacteriophage Phi6, a SARS-CoV-2 surrogate. Performance increase against SARS-CoV-2 is attributed to its higher sensitivity to UVC.

HVAC + UVC							
Sampling Time (Min)	1	2	3	Average (PFU/Gel)	Phi6 LRV	Phi6 Reduction (%)	LRV Extrapolated to SARS-CoV-2
0	$5.30 \times 10^2$	$6.90 \times 10^2$	$6.30 \times 10^2$	$6.17 \times 10^2$	-	-	-
5	$2.00 \times 10^1$	$5.00 \times 10^1$	$2.00 \times 10^1$	$3.00 \times 10^1$	1.31	95.14	3.86
10	$2.00 \times 10^1$	$1.00 \times 10^1$	$1.00 \times 10^1$	$1.33 \times 10^1$	1.67	97.84	6.62
15	$1.00 \times 10^1$	$1.00 \times 10^1$	$1.00 \times 10^1$	$1.00 \times 10^1$	1.79	98.38	9.38
HVAC ONLY							
Sampling time (Min)	1	2	3	Average PFU/gel	Phi6 LRV	Phi6 reduction (%)	LRV extrapolated to SARS-CoV-2
0	$6.80 \times 10^2$	$5.60 \times 10^2$	$6.30 \times 10^2$	$6.23 \times 10^2$	-	-	-
5	$8.00 \times 10^1$	$1.20 \times 10^2$	$1.30 \times 10^2$	$1.10 \times 10^2$	0.75	82.34	0.75
10	$8.00 \times 10^1$	$1.00 \times 10^2$	$7.00 \times 10^1$	$8.33 \times 10^1$	0.87	86.63	0.87
15	$5.00 \times 10^1$	$7.00 \times 10^1$	$7.00 \times 10^1$	$6.33 \times 10^1$	0.99	89.84	0.99

To assess if the HVAC + UVC has significantly lower levels of bacteriophage Phi6 than the HVAC control group, we performed a two-sample one-tailed *t*-test at each time with  $p = 0.05$  as a cut-off to determine if the difference was significant. In the case of a significant improvement, to correct for differences in the susceptibility between SARS-CoV-2 a model will be required. Building on the Kahn-Mariita equivalent ventilation model [23], and taking the assumption that the log of the disinfection rate is linear with fluence, it should be possible to work backward from observed effective equivalent air changes per hour (eACH) to the eACH contribution by UVC [23], then estimate the increased eACH for higher susceptibility of viral particles such as SARS-CoV-2. To do so the eACH must be approximated as an exponential whose coefficients are known in both the case where the UVC is on ( $ACH_{HVAC+UVC}$ ) and off ( $ACH_{HVAC}$ ). In the case of the  $ACH_{HVAC+UVC}$ , the saturation of the measurement requires the exclusion of the 15 min time point. Then, the theoretical maximum ( $ACH_{Max}$ ) where all the virus is removed must be estimated from the flow rate assuming ideal mixing. The increase in susceptibility ( $k$ ) must be known from literature or found via a separate experiment and so results from Ma and Linden [21] were used.

$$ACH_{Adjusted} = (ACH_{MAX} - ACH_{HVAC}) \left( 1 - 10^{k \left( 1 - \log \left( \frac{ACH_{HVAC+UVC} - ACH_{HVAC}}{ACH_{Max}} \right) \right)} \right) + ACH_{HVAC} \quad (3)$$

## 3. Results

### 3.1. Spectral Analysis and Bacteriophage Phi6 Dose Response Curve

The dose response analysis revealed that a dose of 40 mJ/cm<sup>2</sup> is enough to obtain 1.5 LRV (96.83% viral reduction) against bacteriophage Phi6 (Table 1, Figure 5). To determine the susceptibility of bacteriophage Phi6 to 267 nm light via a linear regression of the LRV vs. dose was performed with an intercept set to 0 and obtained a susceptibility constant of 0.0315 cm<sup>2</sup>/mJ and an R<sup>2</sup> value of 0.9943.

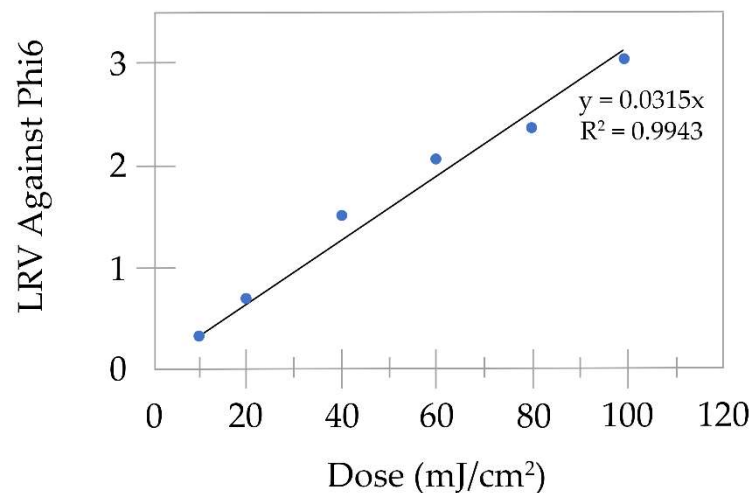


**Figure 5.** The dose response curve of bacteriophage Phi6 as measured against array with peak wavelength of 267 nm in aqueous solution in a Petri dish. Experiments were done in triplicates and means used in graphing.

### 3.2. Modelling and Simulation

The simulation found that the fluence inside of the volume detector inside the cube experienced an average fluence rate of 12.4 mW/cm<sup>2</sup>. The approximate fluence is then 0.05 mJ/cm<sup>2</sup>. The irradiance of light (Figure 6) was consistent with peak measurements from the optometer at 6 mW/cm<sup>2</sup> peak irradiance.

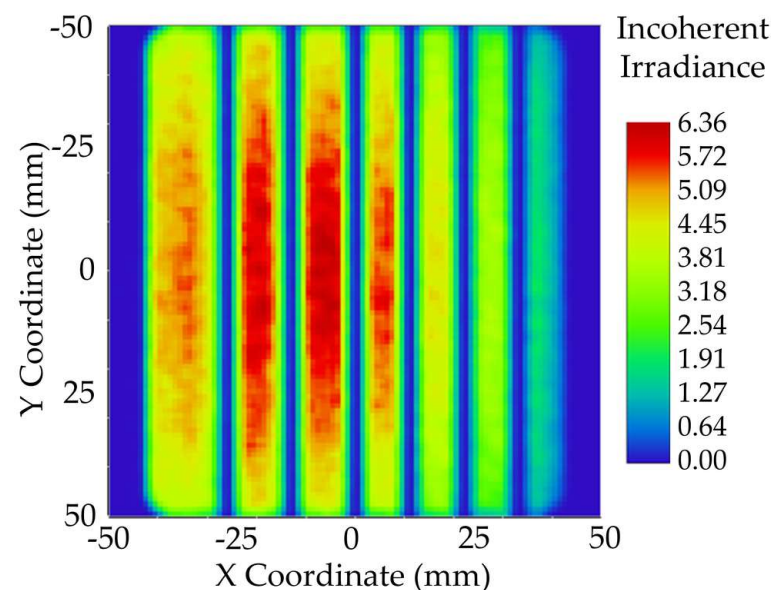


**Figure 6.** A heat map of simulated light escaping from the reaction chamber.

### 3.3. Bacteriophage Phi6 Air Disinfection

The HVAC system complemented with UVC LEDs yielded better results compared to the control HVAC system as shown in Figure 7. The results showed that the HVAC + UVC had significantly lower PFU counts than did the HVAC alone condition in all cases except the initial measurement ( $p = 0.011$  at 5 min,  $p = 0.012$ , at 10 min, and  $p = 0.008$  at 15 min). The HVAC + UVC reduced bacteriophage Phi6 in the cabin by >1 LRV in less than 5 min, while the HVAC alone did not achieve 1 LRV in 15 min. There was a departure from a linear relationship between the dose and the log reduction in the cabin as measured by the samplers (Figure 7). Applying the conversion from bacteriophage Phi6 to SARS-CoV-2 (Figure 8) indicates that SARS-CoV-2 would be reduced by more than a 1 LRV in less than



2 min. To accurately assess both the peak wavelength and the spectral contributions to Phi6 and for extrapolation to SARS-CoV-2 disinfection, the LED spectrum was measured. The peak wavelength was ~267 nm (266.5 nm) and the full width at half maximum (FWHM) was ~11 nm (Figure 8).

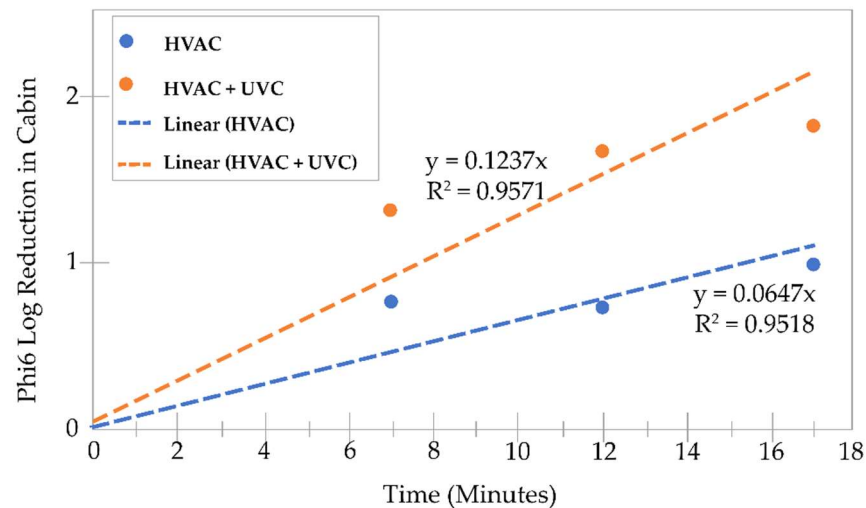


**Figure 7.** A graph of the log reduction in the chamber vs. time. The HVAC + UVC obtained more than 90% viral reduction faster than HVAC only.

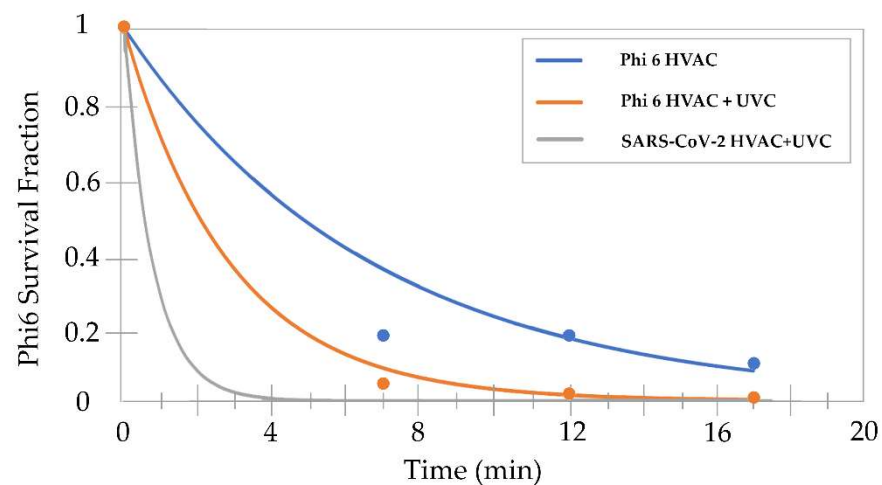


**Figure 8.** Curves of surviving fraction of Phi6 vs. the sampling time. Log fits of the data are shown vs. this data as well as the extrapolation, based on these fits, to the disinfection rate for SARS-CoV-2 which required less time due to wavelength sensitivity.

#### 4. Discussion

Bacteriophage Phi6 has been proposed and used as a surrogate for SARS-CoV-2 [24–26], due to its similar size, shape, envelope, and general features which are like those of pathogenic human viruses such as influenza virus, SARS-CoV-2 and MERS-CoV [24,25,27]. The measured susceptibility of 0.0315 cm<sup>2</sup>/mJ at 267 nm (Figure 9) is close to measurements by Ma and Linden of 0.0315 at 270 nm [21] and of 0.025 cm<sup>2</sup>/mJ at 282 nm [26]. This is 1/15th the susceptibility of SARS-CoV-2 measured as 0.48 cm<sup>2</sup>/mJ at 268 nm by Mariita et al. [28]. Additionally, the susceptibility of microorganisms to UVC varies in air vs. substrates [29]. Microbes are also significantly less susceptible to UVC at higher humidity [30]. Additionally, given the significantly higher UVC resistance of Phi6 compared to SARS-CoV-2 [26], performance against Phi6 can be treated as very conservative. The performance of wide pore filters like in most vehicle HVACs (Heating Ventilation and Air Conditioning) against Phi6 is expected to be relatively like that of SARS-CoV-2 based on its

size and shape [24]. Simulation results of the internal intensity continue to be accurate to around 5% of measured values. Variation may be the result of non-uniformity of the BaSO<sub>4</sub> coating, the coating's variable performance with time, and temperature effects on the LEDs.

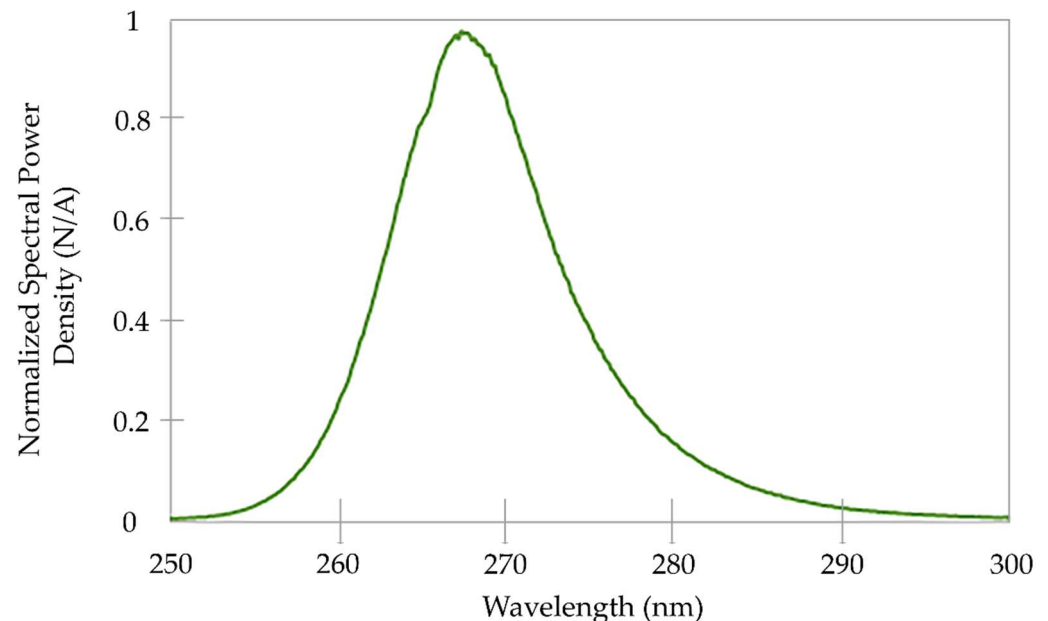


**Figure 9.** The spectrum of the UVC LED used for the generation of dose response curve of Bacteriophage Phi6 with peak emission of 267 nm. The representative spectrum has an FWHM of 11 nm and an asymmetric tail.

The extrapolative model used to estimate the rate of disinfection against SARS-CoV-2 given a known performance against Phi6 found that the time taken to obtain a disinfection of 1 LRV in cabin air was significantly shorter (<2 min) for SARS-CoV-2 than Phi6 (Figure 8). Investigating the parameters revealed that further increases in susceptibility had a negligible impact on the time taken to obtain 1 LRV even with a 10-fold increase in susceptibility. This implies that there is a bottleneck in efficiency at the flow rate of the HVAC and that adding further UVC power to the system would have little benefit. This effect had been previously highlighted by the Kahn-Mariita model to identify design bottlenecks [23].

The rate of disinfection between the middle of the initial sampling point and the 5 min sampling point is higher than between the 5- & 10 min points or the 10- & 15 min points for the HVAC + UVC case. This may be because natural settling is continuing but slowing within the 5 min sampling point or because the measurement has saturated. The HVAC alone data has a similar trend, but it is less pronounced. Because the HVAC alone had lower disinfection, it seems likely that the HVAC only component represents the settling rate component—while the additional deviation in the HVAC + UVC is from the saturation of the measurement. After 15 min in the HVAC + UVC condition, only single plaques were found on the plates further supporting this assessment.

The limited dynamic range of the gel sampling filter limits the ability to measure disinfection rates past 1.7 LRV. It is recommended that development of a high dynamic range method for aerosol sampling using gelatin filters be developed and verified. For vehicle designers and manufacturers, it is also recommended to test in a real vehicle to eliminate all errors from circulation differences and to test with SARS-CoV-2 directly rather than extrapolating. In applications, a wide range of physio-chemical conditions such as relative humidity and temperature of target geographical locations should be factored, optimized, and automated to ensure desired performances. This will require the use of sensors.

Finally, the use of UVC LEDs to complement an automobile HVAC may improve public health by helping inactivate microorganisms [31], including not just bacteria and

viruses, but mold, which is one of the main allergens [32]. Preventing microbial growth in HVAC systems could ensure that the production of volatile organic compounds (VOCs) is not initiated by microorganisms in enclosed spaces [33,34]. UVC can also inactivate dust mites from pets, which can induce rhinitis and asthma attacks [35]. Improving air quality in enclosed spaces through ventilation will alleviate concerns [36].

## 5. Conclusions

The addition of UVC LEDs to a vehicle's HVAC system can allow it to lower Phi6 concentrations in the cabin by more than 1 LRV (90% viral reduction) in less than 5 min, reducing risk of pathogen transmission. Because of wavelength sensitivity, in 5 min, 1 RV (90% reduction) against Phi6 is equivalent to 3.86 LRV (99.986% viral reduction) against SARS-CoV-2. This study demonstrates that UVC can be used to complement existing HVAC systems, ensuring clean cabin air in automobiles.

**Author Contributions:** R.M.M.: conception, design, study coordination, data collection, data analysis, manuscript writing and approved final manuscript. J.H.D.: conception, design, data collection, modeling, data analysis, manuscript writing and approved final manuscript. M.M.L.: data collection, manuscript review, editing and approved final manuscript. R.V.R.: conception, design and approved final manuscript. H.W.: conception, design and approved final manuscript. J.Y.: conception, design and approved final manuscript. All authors have read and agreed to the published version of the manuscript.

**Funding:** This research received no external funding.

**Informed Consent Statement:** Not applicable.

**Data Availability Statement:** All data generated or analyzed during this study are open and publicly available. Raw spectral data can be accessed in FigShare via <https://doi.org/10.6084/m9.figshare.20402649.v1>. Modelling and experiment data can be accessed in FigShare via <https://doi.org/10.6084/m9.figshare.20419854.v1>.

**Acknowledgments:** The authors thank Britt Hafner for his technical assistance and constructive discussions. The authors also thank Kevin Kahn, Sanjay Kamtekar and Jianfeng Chen (Jeff), Patrick Aigeldinger, and Carl Bengtsson for their help with reviewing the manuscript.

**Conflicts of Interest:** All authors work for Crystal IS or its parent company Asahi Kasei. Crystal IS is a UVC LED manufacturer.

## References

1. Bukłaha, A.; Wiczorek, A.; Kruszewska, E.; Majewski, P.; Iwaniuk, D.; Sacha, P.; Tryniszewska, E.; Wiczorek, P. Air Disinfection—From Medical Areas to Vehicle. *Front. Public Health* **2022**, *10*, 820816. Available online: <https://www.frontiersin.org/article/10.3389/fpubh.2022.820816> (accessed on 28 June 2022). [CrossRef] [PubMed]
2. Hurley, K.V.; Wharton, L.; Wheeler, M.J.; Skjøth, C.A.; Niles, C.; Hanson, M.C. Car cabin filters as sampling devices to study bioaerosols using eDNA and microbiological methods. *Aerobiologia* **2019**, *35*, 215–225. [CrossRef]
3. Kim, K.-H.; Kabir, E.; Jahan, S.A. Airborne bioaerosols and their impact on human health. *J. Env. Sci.* **2018**, *67*, 23–35. [CrossRef] [PubMed]
4. Núñez, A.; Amo de Paz, G.; Rastrojo, A.; García Ruiz, A.M.; Alcamí, A.; Gutiérrez-Bustillo, A.M.; Moreno Gómez, D.A. Monitoring of airborne biological particles in outdoor atmosphere. Part 1: Importance, variability and ratios. *Int. Microbiol.* **2016**, *19*, 1–13. [PubMed]
5. Mathai, V.; Das, A.; Bailey, J.A.; Breuer, K. Airflows inside passenger cars and implications for airborne disease transmission. *Sci. Adv.* **2021**, *7*, eabe0166. [CrossRef]
6. Jung, J.H.; Lee, J.E.; Lee, C.H.; Kim, S.S.; Lee, B.U. Treatment of fungal bioaerosols by a high-temperature, short-time process in a continuous-flow system. *Appl. Environ. Microbiol.* **2009**, *75*, 2742–2749. [CrossRef]
7. Abubakar, I.; Tillmann, T.; Banerjee, A. Global, regional, and national age-sex specific all-cause and cause-specific mortality for 240 causes of death, 1990–2013: A systematic analysis for the Global Burden of Disease Study 2013. *Lancet* **2015**, *385*, 117–171.
8. Drenik, G. The Air Inside Our Car Is More Dangerous Than The Outside Air: CabinAir Is Fixing This. *Forbes*. Available online: <https://www.forbes.com/sites/garydrenik/2021/05/27/the-air-inside-our-car-is-more-dangerous-than-the-outside-air-cabinair-is-fixing-this/> (accessed on 20 July 2022).

9. Gross, A. Think You're In Your Car More? You're Right. Americans Spend 70 Billion Hours Behind the Wheel. *AAA Newsroom* 2019. Available online: <https://newsroom.aaa.com/2019/02/think-youre-in-your-car-more-youre-right-americans-spend-70-billion-hours-behind-the-wheel/> (accessed on 18 July 2022).
10. Asahi Kasei America. Clean Surfaces and Safe In-Cabin Air—New Global Survey by Asahi Kasei Shows Growing Need for Hygienic Automotive Interiors. 2021. Available online: <https://www.businesswire.com/news/home/20210504005096/en/Clean-Surfaces-and-Safe-In-Cabin-Air-%E2%80%93-New-Global-Survey-by-Asahi-Kasei-Shows-Growing-Need-for-Hygienic-Automotive-Interiors> (accessed on 18 July 2022).
11. Hattrup-Silberberg, M.; Hausler, S.; Heineke, K.; Laverty, N.; Möller, T.; Schwedhelm, D.; Wu, T. Five COVID-19 Aftershocks Reshaping Mobility's Future | McKinsey. 2020. Available online: <https://www.mckinsey.com/industries/automotive-and-assembly/our-insights/five-covid-19-aftershocks-reshaping-mobilitys-future> (accessed on 29 June 2022).
12. Motavalli, J. Drive Smart: 20 Ways to Save Gas. *Forbes Wheels* 2022. Available online: <https://www.forbes.com/wheels/advice/gas-saving-tips/> (accessed on 1 August 2022).
13. Fontaras, G.; Zacharof, N.-G.; Ciuffo, B. Fuel consumption and CO<sub>2</sub> emissions from passenger cars in Europe—Laboratory versus real-world emissions. *Prog. Energy Combust. Sci.* **2017**, *60*, 97–131. [CrossRef]
14. Nazarious, M.I.; Mathanlal, T.; Zorzano, M.-P.; Martin-Torres, J. Pressure Optimized PowEred Respirator (PROPER): A miniaturized wearable cleanroom and biosafety system for aerially transmitted viral infections such as COVID-19. *HardwareX* **2020**, *8*, e00144. [CrossRef]
15. Mariita, R.M.; Randive, R.V.; Lottridge, M.M.; Davis, J.H.; Bryson, B.W. UVC Inactivation of Black Mold is Wavelength-Dependent, and its Growth in HVAC Systems is Preventable Using Periodic Dosing with commercially available UVC LEDs. *bioRxiv* **2022**, 1–20. [CrossRef]
16. Bono, N.; Ponti, F.; Punta, C.; Candiani, G. Effect of UV Irradiation and TiO<sub>2</sub>-Photocatalysis on Airborne Bacteria and Viruses: An Overview. *Materials* **2021**, *14*, 1075. [CrossRef] [PubMed]
17. Chen, Y. Pros and Cons of UVC LEDs and Lamps for Disinfecting Applications. Available online: <https://www.ledinside.com/news/2020/8/uv-light-comparison> (accessed on 3 August 2022).
18. Randive, R.; Mariita, R.; Davis, J.; Schwegler, T.; Franchy, M.; Kamtekar, S.; Rother, H. Demonstrating UVC LEDs inside Automobile HVAC Chambers for Clean Cabin Air and Airborne Transmission Risk Reduction. Warrendale, PA: SAE Technical Paper 2022. Available online: <https://www.sae.org/publications/technical-papers/content/2022-01-0197/> (accessed on 18 July 2022).
19. Kim, S.C.; Kang, S.; Lee, H.; Kwak, D.-B.; Ou, Q.; Pei, C.; Pui, D.Y.H. Nanofiber Filter Performance Improvement: Nanofiber Layer Uniformity and Branched Nanofiber. *Aerosol Air Qual. Res.* **2020**, *20*, 80–88. [CrossRef]
20. Van Doremalen, N.; Bushmaker, T.; Morris, D.H.; Holbrook, M.G.; Gamble, A.; Williamson, B.N.; Tamin, A.; Harcourt, J.L.; Thornburg, N.J.; Gerber, S.I.; et al. Aerosol and Surface Stability of SARS-CoV-2 as Compared with SARS-CoV-1. *N. Engl. J. Med.* **2020**, *382*, 1564–1567. [CrossRef] [PubMed]
21. Ma Ben Gundy Patricia, M.; Gerba Charles, P.; Sobsey Mark, D.; Linden Karl, G.; Dudley Edward, G. UV Inactivation of SARS-CoV-2 across the UVC Spectrum: KrCl\* Excimer, Mercury-Vapor, and Light-Emitting-Diode (LED) Sources. *Appl. Environ. Microbiol.* **2021**, *87*, e01532-21. [CrossRef]
22. Bangiyev, R.; Chudaev, M.; Schaffner, D.W.; Goldman, E. Higher Concentrations of Bacterial Enveloped Virus Phi6 Can Protect the Virus from Environmental Decay. *Appl. Env. Microbiol.* **2021**, *87*, e0137121. [CrossRef]
23. Kahn, K.; Mariita, R.M. Quantifying the Impact of Ultraviolet Subtype C in Reducing Airborne Pathogen Transmission and Improving Energy Efficiency in Healthy Buildings: A Kahn–Mariita Equivalent Ventilation Model. *Front. Built Environ.* **2021**, *7*, 725624. [CrossRef]
24. Barros, J.; Ferraz, M.P.; Monteiro, F.J. Bacteriophage Phi 6 as Surrogate and Human-Harmless Viruses to Study Anti-SARS-CoV-2 Approaches. *Int. J. Mol. Sci.* **2021**, *2*, 175–177.
25. Fedorenko, A.; Grinberg, M.; Orevi, T.; Kashtan, N. Survival of the enveloped bacteriophage Phi6 (a surrogate for SARS-CoV-2) in evaporated saliva microdroplets deposited on glass surfaces. *Sci. Rep.* **2020**, *10*, 22419. [CrossRef]
26. Ma, B.; Linden, Y.S.; Gundy, P.M.; Gerba, C.P.; Sobsey, M.D.; Linden, K.G. Inactivation of Coronaviruses and Phage Phi6 from Irradiation across UVC Wavelengths. *Env. Sci. Technol. Lett.* **2021**, *8*, 425–430. [CrossRef]
27. Serrano-Aroca, Á. Antiviral Characterization of Advanced Materials: Use of Bacteriophage Phi 6 as Surrogate of Enveloped Viruses Such as SARS-CoV-2. *Int. J. Mol. Sci.* **2022**, *23*, 5335. [CrossRef]
28. Mariita, R.M.; Peterson, J.W. Not all wavelengths are created equal: Disinfection of SARS-CoV-2 using UVC radiation is wavelength-dependent. *Access Microbiol.* **2021**, *3*, 000276. [CrossRef] [PubMed]
29. Brickner, P.W.; Vincent, R.L.; First, M.; Nardell, E.; Murray, M.; Kaufman, W. The Application of Ultraviolet Germicidal Irradiation to Control Transmission of Airborne Disease: Bioterrorism Countermeasure. *Public Health Rep.* **2003**, *118*, 99–114. [CrossRef]
30. Reed, N.G. The history of ultraviolet germicidal irradiation for air disinfection. *Public Health Rep.* **2010**, *125*, 15–27. [CrossRef] [PubMed]
31. Lutz, E.A.; Sharma, S.; Casto, B.; Needham, G.; Buckley, T.J. Effectiveness of UV-C equipped vacuum at reducing culturable surface-bound microorganisms on carpets. *Env. Sci. Technol.* **2010**, *44*, 9451–9455. [CrossRef] [PubMed]
32. Bernstein, J.A.; Bobbitt, R.C.; Levin, L.; Floyd, R.; Crandall, M.S.; Shalwitz, R.A.; Seth, A.; Glazman, M. Health Effects of Ultraviolet Irradiation in Asthmatic Children's Homes. *J. Asthma* **2006**, *43*, 255–262. [CrossRef] [PubMed]

- 
33. Cone, M. Volatile Organic Compounds May Worsen Allergies and Asthma. *Scientific American*. Available online: <https://www.scientificamerican.com/article/volatile-organic-compounds/> (accessed on 20 July 2022).
  34. Liu, C.-Y.; Tseng, C.-H.; Wang, H.-C.; Dai, C.-F.; Shih, Y.-H. The Study of an Ultraviolet Radiation Technique for Removal of the Indoor Air Volatile Organic Compounds and Bioaerosol. *Int. J. Environ. Res. Public Health* **2019**, *16*, 2557. [[CrossRef](#)] [[PubMed](#)]
  35. Lah, E.F.C.; Musa, R.N.A.R.; Ming, H.T. Effect of germicidal UV-C light (254 nm) on eggs and adult of house dustmites, *Dermatophagoides pteronyssinus* and *Dermatophagoides farinae* (Astigmata: Pyroglyphidae). *Asian Pac. J. Trop. Biomed.* **2012**, *2*, 679–683. [[CrossRef](#)]
  36. Bower, J. Chapter 5: Indoor Air Pollutants and Toxic Materials | Healthy Housing Reference Manual | NCEH. 2019. Available online: <https://www.cdc.gov/nceh/publications/books/housing/cha05.htm> (accessed on 3 August 2022).